Journal of Sciences, Islamic Republic of Iran 14(1): 37-52 (2003)
National Center For Scientific Research, ISSN 1016-1104

MODELLING THE As-Au ASSOCIATION IN HYDROTHERMAL GOLD MINERALIZATION: EXAMPLE OF ZARSHURAN DEPOSIT, NW IRAN

B. Mehrabi[1,*], B.W.D. Yardley[2], and A. Komninue[3]

[1] *Department of Geology, Tarbiat Moalem University, No. 49, Mofateh Ave., Tehran 15614, Islamic Republic of Iran*
[2] *School of Earth Sciences, University of Leeds, Leeds LS2 9JE, England*
[3] *Anthias 18-20, Ano Kyseli, Athens 11346, Greece*

Abstract

The paragenetic sequence at the Zarshuran arsenic deposit, NW Iran demonstrates that during the late stage of mineralization, gold precipitated with orpiment, realgar and arsenian pyrite. Thermodynamic calculations have been used to model sulphur and arsenic speciation and solubility at the P-T conditions of the late stage mineralization, reconstructed based on fluid inclusion studies. Arsenic was probably transported as the As^{+3} complex; $H_3AsO_3^0$, while the dominant Au complex was $Au(HS)_2^-$. The calculations indicate that both pH and fO_2 have opposing effects on gold and arsenic solubilities. Hence co-precipitation was not simply a response to changes in pH and fO_2. Experimental data and geochemical modelling results indicate that pH, fO_2, P, T and S availability are the main equilibrium factors controlling gold and arsenic transport and precipitation. The proposed geochemical model suggests that partial reduction of an oxidizing As-rich fluid of partial magmatic origin (As~S), leached gold from the Precambrian metamorphic rocks as it was reduced, but further reduction by the black shale resulted in gold and arsenic co-precipitation. An alternative model for As and Au co-precipitation is a kinetic one, with Au being adsorbed onto growing orpiment surfaces despite being undersaturated in the fluid. The result shows the condition in which an arsenic saturated fluid with mAs=mS may persist to a point where gold bisulphide has maximum solubility, and so may leach gold. Further reduction from that point may causes gold and orpiment co-precipitation. The high level As to S concentrations is one of the main features here, and is not known for the Zarshuran fluid, although data from different magmatic sources suggest that the requirements are within the range of magmatic fluids.

Keywords: Geochemical modelling; Au-As association; Zarshuran deposit; Orpiment; Gold

Introduction

Geochemical modelling has become an increasingly important tool for understanding ore genesis. This approach is most effective in those cases where the ore fluid can be analysed directly (*e.g.* the study of a Broadlands-Type epithermal ore fluid by Spycher and Reed, [47]). In other cases, it is more difficult due to the number of assumptions about the ore fluid(s) that must be made. The characteristics of ore fluids that formed

* *E-mail: mehrabi@saba.tmu.ac.ir*

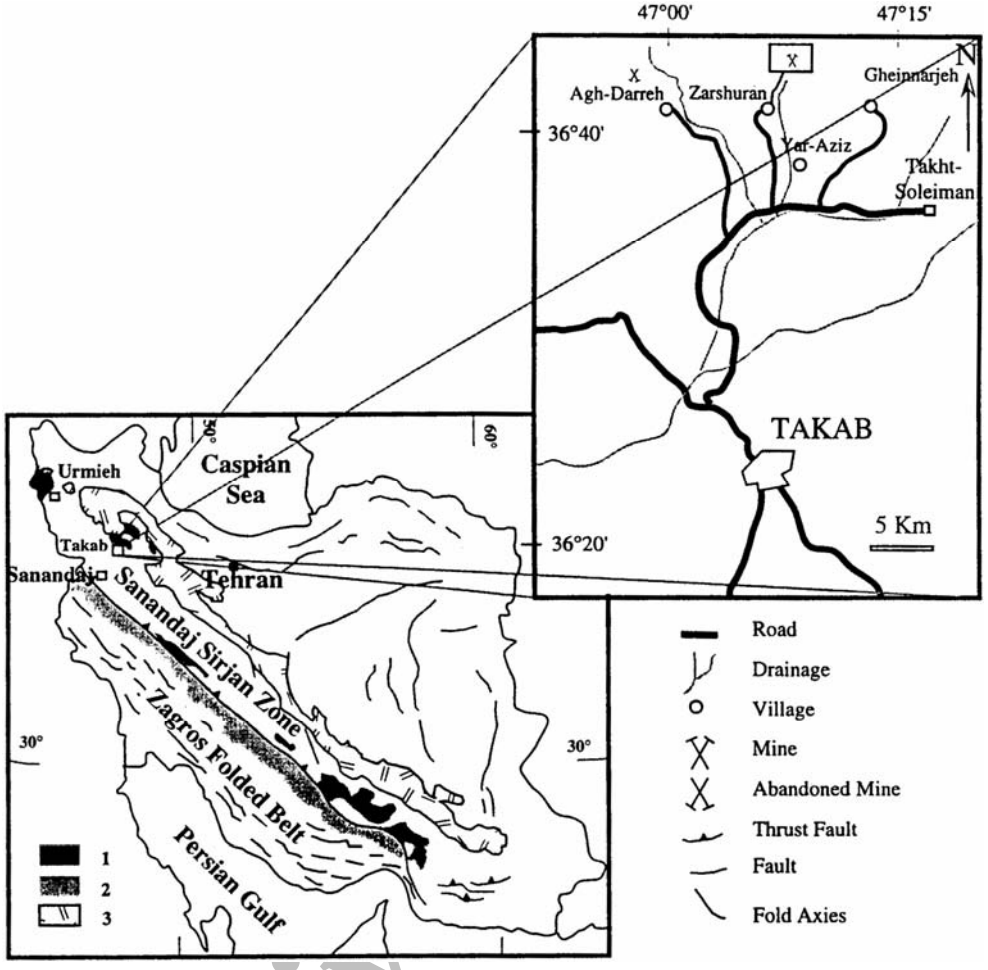

Figure 1. Location map of the Zarshuran deposit and its relation to the Zagros subdivision and the Tertiary volcanic belt according to Stocklin [48]. 1: Precambrian basement, 2: Zagros thrust zone and 3: Tertiary volcanic belt.

fossil systems can however be characterized by fluid inclusion analysis and from mineral assemblages. However these do not necessarily define the original ore fluid but rather one which had already interacted to an unknown extent with the host rocks.

The main purpose of this paper is to examine the mechanism of transport and deposition of associated gold and arsenic sulphides, which are the main ores at the Zarshuran deposit, NW Iran. An attempt has been made to calculate gold and arsenic solubility under P-T conditions close to those inferred for arsenic sulphide deposition at Zarshuran, and to find the likely causes of gold and orpiment co-precipitation. The effect of pH, oxygen fugacity and ligand concentration on orpiment and gold solubility at 1 kb and 185°C has been calculated using the codes "EQ36NR" (modified by A. Komninou) and "SUPCRT92" [20]. Thermodynamic data from SUPCRT92 and other sources was incorporated in an appropriate EQ36NR database valid at 1 kb.

Zarshuran Hydrothermal Mineralization

The Zarshuran deposit is located at 36° 43.4' N 47° 08.2' E, 42 km north of the town of Takab in West Azarbaijan province, NW Iran (Fig. 1). The Zarshuran is well known in Iran for arsenic mining, orpiment and realgar having been worked for hundreds of years, but is now of interest as a gold prospect. Zarshuran deposit was almost certainly mined for gold also in ancient times; large piles of rocks at four sites in drainage downstream along the Zarshuran river have been interpreted as products of alluvial mining [30,40]. Old workings and trenches in the area seem to be the remains of ancient gold mining [40]. The geology and mineralization of the Zarshuran deposit are described in [3,24,25].

The mining area is on the south limb of the Iman Khan anticline, a structure cored by the Precambrian metamorphic basement with late Precambrian carbonates and shales. These are overlained by Cambro-Ordovician biomicrite limestone and dolomite. Tertiary (Oligocene) rocks transgress with a basal conglomerate, marl, tuff and sandstone [40]. Miocene volcanics, mainly andesite and rhyolite, disconformably overly the Oligo-Miocene formations. A shallow dipping travertine of Quaternary age is exposed in several places in the area.

The gold and arsenic mineralization at the Zarshuran deposit is semi-conformable within the presumed late Precambrian Zarshuran Black Shale Unit, along a strike length of 1 km, and dips approximately 35-50° SW. The Zarshuran Unit is exposed for about 5 km and mineralization has been reported to occur to different degrees in different parts of this unit [40]. The thickness of the mineralized zone varies between 5-60 m with an average of 15-20 m. The main arsenic mineralization is in the form of a series of anastamosing pods, lenses and veins; the average thickness of the lenses is c. 1 m.

The mineral assemblage includes micron to angstrom-size gold, orpiment, realgar, stibnite, getchellite, cinnabar, thallium minerals, barite, Au-As-bearing pyrite, base metal sulphides and sulphosalts. Most of the gold is detectable only by chemical analysis, but sparse metallic gold has been observed in hydrothermal quartz, orpiment and realgar (Fig. 2). Electron microprobe and bulk chemical analysis indicate that gold probably occurs in minerals such as pyrite-arsenian pyrite, orpiment and realgar, although the nature of gold occurrence in these phases is still unknown.

Hydrothermal alteration features associated with mineralization include, 1) decalcification, 2) silicification, 3) argillization, 4) dolomitization, 5) minor oxidation and acid leaching and 6) supergene alteration.

Geochronologic studies utilizing K/Ar and Ar/Ar techniques on hydrothermal argillic alteration and on volcanic rocks, indicate that mineralization at Zarshuran formed at 14.2±0.4 Ma, and was contemporaneous with nearby Miocene volcanic activity, 13.7±2.9 Ma [25].

The main characteristic features of mineralization at Zarshuran are: a) submicron to micron size disseminated gold, b) calcareous and carbonaceous shale and limestone host rocks, c) presence of a typically epithermal element suite of As-Sb-Hg-Tl associated with the gold, and d) associated decalcification, silicification and argillization of wall rocks. These features are similar to those of the sediment-hosted gold deposits of the "Carlin-type", in the Great Basin of western North America.

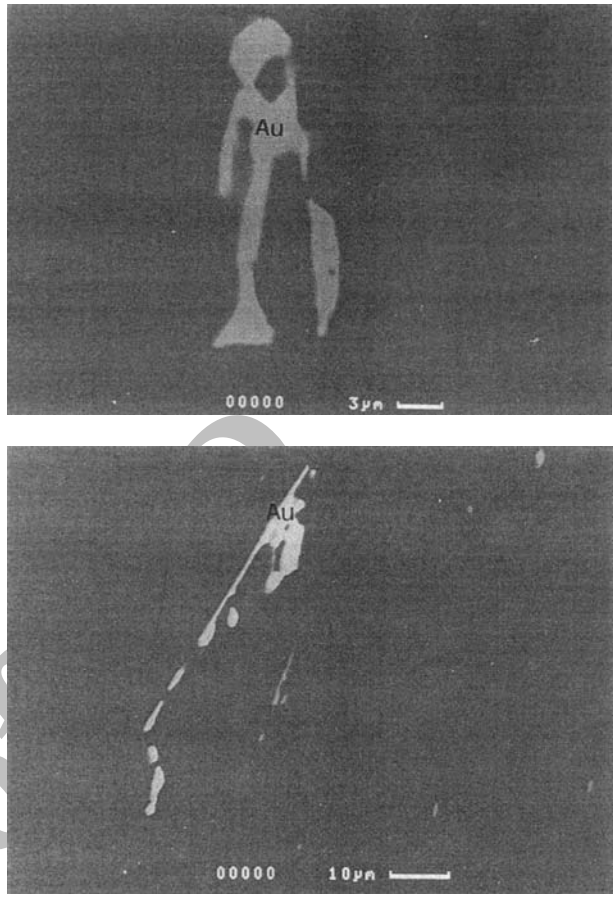

Figure 2. BSE photograph of metallic gold (bright colour) in orpiment (dark colour) from the Zarshuran deposit.

Fluid Inclusion Studies

Fluid inclusion studies [24] indicate the presence of at least two types of fluids at the Zarshuran deposit; 1) gas-rich fluid (mainly CO_2-bearing) associated with moderate salinity and high temperature aqueous fluid, and 2) aqueous fluids of varying salinity and homogenization temperature.

Orpiment is mainly associated with quartz and to a lesser extent with fluorite±sphalerite. These occurrences yield different generations of two-phase and one-phase inclusions. Fluorite shows optical and cathodoluminescence oscillatory growth zoning, which helps to identified primary inclusions clearly. One-phase inclusions are mainly high density CH_4±CO_2 and nucleate bubbles on cooling below −82.4°C. However a group of medium relief, dark, single phase inclusions with triple point melting between −57.1 to −57.8°C homogenize to liquid between +9 to +14.2°C and are located in the same pseudosecondary planes as the methane inclusions, but are predominantly of CO_2.

Two-phase water inclusions of primary, pseudo-secondary and secondary origins were found in the same vein samples.

Due to the multiple generations and wide variety of inclusion composition, it is difficult to identify primary inclusions, except in zoned fluorite crystals. Two groups of primary water inclusions were identified in fluorite. The first group has a high salinity fluid (Tm −18.6 to −24.8°C) with homogenization temperatures of 129 to 197°C. The second group is of relatively low salinity (Tm −7.8 to −9.6°C) and homogenizes between 128 and 236°C (Fig. 3). Orpiment and quartz veins and patches contain primary inclusions with Tm between −4.6 to −6.8°C and Th between 149 to 162°C. These inclusion are paragenetically related to the end of the late stage of mineralization.

Pseudosecondary aqueous inclusions are the most abundant type present in orpiment and fluorite. The pseudosecondary inclusions can be divided into three groups based on the Th/Tm diagram (Fig. 3). The first group is of relatively high salinity (Tm −8.1 to −12.3°C), with homogenization temperatures of 161 to 239°C. The second group has lower salinity (Tm −6.2 to −3.4°C) and scattered homogenization temperatures (Th 124 to 244°C). The third group is very low salinity, near to pure water (Tm −2.8 to −0.2°C), with low homogenization temperature (Th 129.5 to 142°C).

Secondary inclusions have similar characteristics to the second group of pseudosecondary inclusions, though they show less variation in homogenization temperature (Fig. 3A).

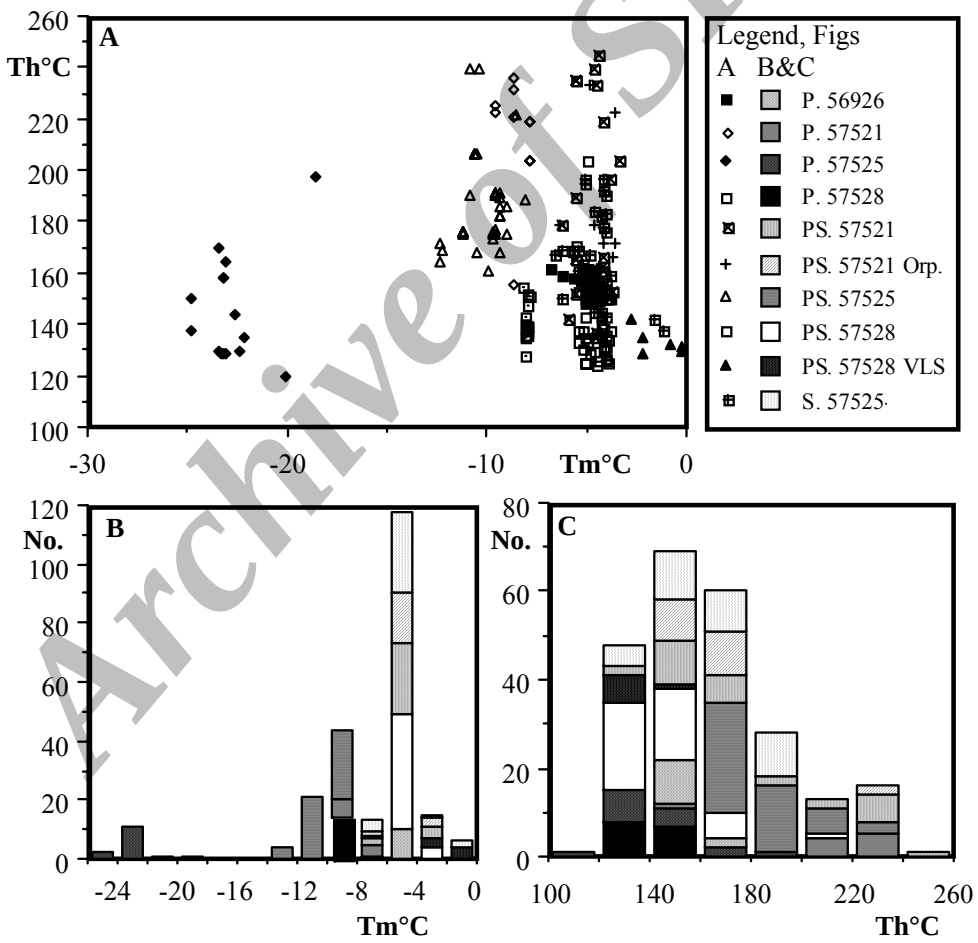

Figure 3. Properties of two-phase aqueous fluids: A) Th/Tm diagram; B) final ice melting histogram and C) homogenization temperature histogram. The very high salinity primary inclusions in fluorite might be locally derived fluids (sample 57525). Very low salinity (VLS) and low temperature fluids (PS. 57528 VLS and S. 57525) may represent a meteoric water end member. Abbreviations: P. = Primary, PS. = Pseudosecondary, S. = Secondary, Orp. = Orpiment-hosted.

Contemporaneous CH_4, CO_2 and H_2O inclusions in sample 57528 provide good constraints on the P-T conditions. Figure 4A shows the isochores of P-T condition reconstructed from them. The inferred P-T conditions are 865±375 bars and 185±40°C. In addition sample 57521 yielded both gas and water inclusions, but the phase changes in the CH_4 inclusions were not observed clearly, mainly due to the presence of fibrous solid phase. The inferred P-T condition based on CO_2 and H_2O fluid inclusions are 1175±225 bars and 220±35°C (Fig. 4B).

The inferred data for pressure and temperature of the inclusion pairs are probably spread around the true values. It is more likely that fluid pressure fluctuation caused variation in fluid densities than temperature changes.

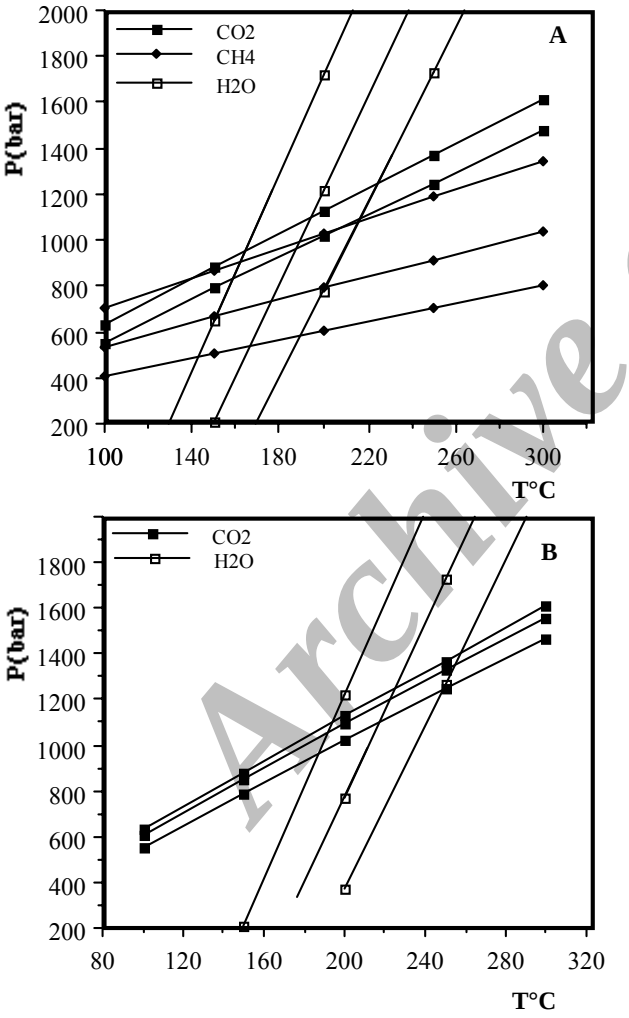

Figure 4. P-T conditions during arsenic mineralization estimated by the intersecting isochores method: A) P-T based on CO_2, CH_4 and H_2O fluid inclusions in sample 57528, B) P-T based on CO_2 and H_2O fluid inclusions in sample 57521.

The trapping pressure of 945±455 bars for gold mineralization at the Zarshuran can be converted to a depth of formation based on either lithostatic or hydrostatic fluid pressure. A typical lithostatic pressure gradient of 250 bars/km requires a depth of 3.8±1.8 km to reach the estimated pressure. On the other hand, if the pressure was hydrostatic, a depth of 11.8±5.7 km in hot hydrostatic or 9.45±4.55 km in cold hydrostatic condition is required to attain the measured pressure.

The estimated depth based on a hydrostatic regime is geologically unreasonable, in view of the likely cover over the region at the time of its formation. On the other hand hydrothermal mineral deposition under lithostatic pressure conditions is problematic, because overpressures generally reflect very low permeability so that fluids cannot circulate. An abrupt transition from hydrostatic pressure to perhaps 80 to 85 percent lithostatic pressure, which is a typical gradient for vertical crack formation by overpressured fluid in laterally stressed rock [10,12], would permit fluid migration at the estimated pressures.

Fluid inclusions of varying salinity and Th at the Zarshuran deposit nevertheless exhibit similar petrographic features, so the observed variations in salinity probably represent the original compositional variation in the hydrothermal system. Mechanisms which could produce this variations include; 1) boiling, 2) water/rock reactions and 3) fluid mixing.

Boiling is commonly cited to explain increases in salinity. However neither vapour inclusions nor homogenization to vapour phase have been observed at Zarshuran. Furthermore, the inferred pressure of entrapment (945±445 bar) is outside the two-phase region for H_2O-NaCl-CO_2 fluids at the inferred temperature.

Water-rock interaction is another possible mechanism for increasing fluid salinity, either by leaching Cl or removing H_2O from the fluid. There is evidence of widespread wall rock alteration including, decalcification, silicification, argillization and dolomitization. However low water:rock ratios are required for alteration to modify salinity, and this is unlikely for such heavily mineralized rocks.

Very simple origin salinity variation may simply result from mixing of two or more fluids. The presence of very low salinity, low temperature fluids and moderate to high salinity fluids trapped at variable temperatures may reflect the end members of the fluids involved in the system, for example meteoric water and magmatic gas input.

Au-As Association in Sedimentary Hosted Disseminated Gold Deposits (SHDGD)

The association of gold and arsenic in ore deposits and geothermal system is well known [22,53,55], although the causes of it are not well understood. Reviewing the pre-1979 literature, Boyle [6] concluded that arsenic is one of the best pathfinders for gold and recent publications are in full agreement with that.

The well-known deposit-scale correlation between As-Au in sediment-hosted disseminated gold deposits (SHDGD) has been the basis of much geochemical prospecting [2]. However, little information is available on the association of these elements at the grain-scale. The common view is that gold in SHDGD is associated with As and is mainly present in arsenian pyrite [2,54]. Orpiment, realgar and arsenopyrite are common constituents of the ore in SHDGD, but do not normally contain levels of gold greatly above those found in the same minerals where they are not from gold deposits [2].

In contrast, in the Zarshuran deposit there is a spatial correlation of orpiment with gold and in addition to native gold (Fig. 2), chemical analysis of nearly pure orpiment shows up to 2 ppm Au [24].

Hydrothermal Transport of Arsenic and Gold

Arsenic oxide (As_2O_3) is very soluble, especially in alkaline solution. The solubility of orpiment (As_2S_3) in water and sulphide-bearing fluids has been measured by Miranova and Zotov [27], Miranova *et al.* [29] and Webster [52]. Orpiment solubility experiments in a variety of salt- and sulphide-bearing solutions have identified a large number of As-complexes, summarized by Webster [52]. The thermodynamic properties of arsenic aqueous species in the As(III)-S(II)-O-H system [1] indicate that at temperatures below 150°C, and at high sulphide content, the dominant arsenic species in solution are $As_2S_3^{0}{}_{(aq)}$ (low pH), $HAs_2S_4^{-}$ (intermediate pH), and $As_2S_4^{2-}$ (alkaline conditions). At temperatures of 150-200°C and above, the major form of arsenic in hydrothermal solution is $H_3AsO_3^{0}{}_{(aq)}$ [63], even where sulphide is still present. Thus in acid or near neutral conditions, arsenian acid ($H_3AsO_3^{0}$) is considered to be the main product of both As_2S_3 and As_2O_3 dissolution [18,28,32], and has been incorporated in the modelling carried out here with data from Zotov *et al.* [63].

Gold has been recovered from a wide range of hydrothermal deposits, formed under different physiochemical conditions and from fluids of different chemistry. Such a wide range of environments indicates that there maybe several types of aqueous gold complexes and that the complexing depends on temperature, pH, redox state and ligand concentration of hydrothermal fluids [13].

Chloride and bisulphide complexes of gold have been studied by Seward [42], Henley [15], Renders and Seward [35] Hayashi and Ohmoto [13] and Gammons and Williams-Jones [11]. Russian data on gold complexing and solubilities is reviewed and summarized by Zotov *et al.* [63].

Seward [42] was the first to demonstrate that sulphide complexes of gold(I) were of major importance in transport and deposition of gold by hydrothermal fluids. His experiments extended from 160 to 300°C and up to 1.5 kb, and showed that three complexes, $AuHS^{0}$ (acid pH), $Au(HS)_2^{-}$ (near-neutral to weakly alkaline), and $Au_2(HS_2)S_2^{-}$ (alkaline pH), were present in aqueous sulphide solutions.

The experimental studies on gold solubility in NaCl- and H_2S-bearing solution at 250-350°C by Hayashi and Ohmoto [13] indicated that gold solubility is independent of the activity of Cl^{-} in the solution suggesting that chloride complexes are not important in those conditions, but in detail their results are inconsistent with Renders and Seward [36], Zotov *et al.* [63] and Gammons and Williams-Jones [11]. The Gammons and Williams-Jones [11] study of stability of Au(I) chloride complexes in hydrothermal fluid at 300°C indicated that $AuCl_2^{-}$ may be an important agent of Au transport at T > 300°C, or in highly oxidized fluids. Zotov *et al.* [63], reviewing their earlier work, have shown that gold also becomes quite soluble as $Au(OH)^{0}$ in highly oxidized fluids. There is a general consensus that most Au deposits form from H_2S-rich fluids in which Au(I) bisulphide complexes play a dominant role [44], however there are examples of ore deposits in which chloride complexes may have been more important [11]. These include in particular, porphyry Au-Cu deposits associated with alkaline magmas [50], and low temperature hydrothermal deposits formed from oxidized brines (*e.g.* Coronation Hill, Australia; [26]). The Au-U association of some hydrothermal deposit implies that transport of Au in oxidized fluid as $Au(OH)^{0}$ may also be important [4].

The close geochemical association of arsenic with gold has led to the speculation that arsenothio, $Au(AsS_2)^{0}$ and $Au(AsS_3)^{2-}$, complexes may be important in gold transport [42]. To evaluate the importance of arsenothio complex, Rytuba [38] measured the combined solubility of orpiment and gold in 1 m NaCl solution up to 300°C and found the gold solubility is less than 50 ppb.

As Concentration in Magmatic Fluids

The association of the Zarshuran mineralization with contemporaneous Miocene volcanic activity, the presence of gold and antimony mineralization in quartz veins hosted by Miocene volcanic rocks, the abundant arsenic mineralization and the gas-rich fluid inclusions, suggest that a magmatic input is important for the Zarshuran hydrothermal mineralization [24]. Although it is likely that As and Sb were introduced from a magmatic source, data on their concentrations in magmatic fluid is scarce.

Studies by Pike [33] of fluid inclusions in the quartz cores of Li-pegmatites from southern Africa, showed that arsenic and antimony daughter minerals may occur within CO_2-bearing primary fluid inclusions (Fig. 5) while crush leach analysis yielded very high As level in some fluids (Table 1). He reported up to 2117 ppm As but pointed out that due to the presence of dilute aqueous secondary fluid inclusions in the bulk samples analysed, the arsenic concentration in the CO_2-bearing fluids may have been much higher than this. The data yield average concentrations of 9.42×10^{-3} m As and 1.65×10^{-2} m SO_4 in these magma-derived pegmatite fluids.

Arsenic can also reach significant concentration (up to 12 ppm) in geothermal waters (Table 2), where it is also often of likely magmatic origin. Even where the magmatic source is far from proven, fluid associated with gold mineralization may have high As levels. Yardley *et al.* [62] found that fluid inclusions from mesothermal gold quartz veins with associated arsenopyrite contained 0.0005 to 0.0030 m As and 0.0016 to 0.0121 SO_4 (Table 1). In the light of this data and the extensive occurrence of As-minerals at Zarshuran and other SHDGD, it seems likely that As may be a major fluid component.

Geochemical Modelling of Equilibrium Factor

Thermodynamic data for arsenic, gold and sulphur aqueous species, minerals and gases are not entirely consistent, therefore the first step was an examination of the published data. Thermodynamic data were selected as follows: sulphides from Helgeson *et al.* [14]; arsenic aqueous species and minerals from Zotov *et al.* [63]; and gold hydrosulphides species from Benning and Seward [5] used dissociation constant for H_2S from Ellis and Giggenbach [9] which are different from the earlier data selected by Helgeson *et al.* [14]. For this work, log K values for Au-species were generated from the Benning and Seward [5] experiments to be consistent with Helgeson *et al.* [14] H_2S data.

All aqueous speciation and calculation were carried out using the computer program "EQ36NR" [57-61], modified by A. Komninou (coauthor). The log K values for equilibrium involving sulphur and metal species (Table 3) at a temperature around 185°C and 1 kb, were calculated using SUPCRT92 [20] and input to the EQ36NR database. The temperature and pressure of 185°C and 1 kb used for modelling, were derived from fluid inclusion data.

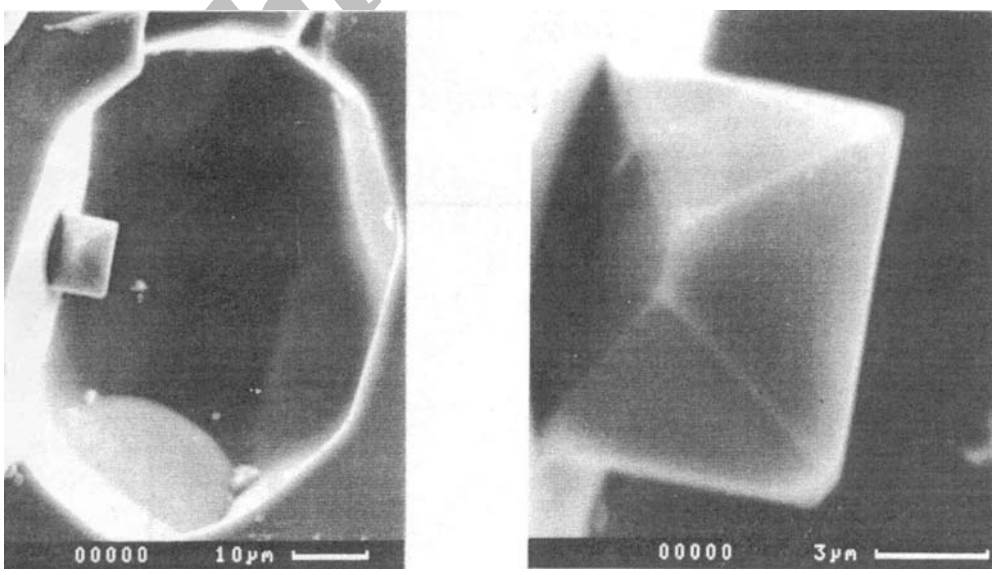

Figure 5. SEM image of fluid inclusion (CO_2-H_2O) containing an arsenic daughter crystal in the cavity, Muiane pegmatite, Mozambique [33].

Table 1. Crush leach data (molality) of arsenic-rich fluids in pegmatitic quartz veins [33]

	50700M	**50707S**	**LD659**	**LD671**	**LD872**	**LD886**	**LD888B**	**LD910**
CO_2	2.92149		2.502	2.265	5.512	4.716	4.440	2.189
Na	0.45021	2.02097	0.879	0.865	0.910	0.925	0.910	0.943
K	0.02069	0.22142	0.026	0.075	0.003	0.032	0.026	0.030
Cs	0.00650	0.00016						
Ca		0.27502	0.023	0.028	0.030	0.021	0.029	0.042
Mg			0.0065	0.0041	0.0006	0.00067	0.0046	0.0029
Fe	0.00205	0.01743	0.0004	0.0014	0.0039	0.0027	0.0014	0.0014
Mn	0.00028	0.01476	0.00005	0.00009	0.00007	0.00012	0.00019	0.00012
Al	0.15357	0.03609	0.012	0.029	0.055	0.016	0.048	0.014
Li	0.87853	0.02222	0.005	0.013	0.069	0.044	0.039	0.009
Sr		0.00402	0.0007		0.0005	0.0008	0.0006	0.0006
Ba	0.00125	0.00202	0.0002	0.0006	0.0003	0.0004	0.0004	0.0002
Cu	0.00067		0.00007	0.00014	0.00021	0.00050	0.00015	0.00005
Zn	0.00679	0.01223	0.00003	0.00059	0.00200	0.00067	0.00034	0.00033
Pb	0.00059	0.00083	0.00001				0.00010	0.00001
As	0.02221	0.01823	0.0015	0.0005	0.0030	0.0025	0.0019	0.0007
Be	0.00039	0.00747						
Bi		2.11E-5						
B	0.17511	0.04116	0.047	0.042	0.053	0.066	0.047	0.042
Cl	0.61807	3.01786	0.703	0.677	0.669	0.680	0.654	0.656
Br	0.00136	0.00496	0.0015	0.0012	0.0011	0.0011	0.0013	0.0015
F			0.043	0.022	0.064	0.028	0.068	0.037
SO_4	0.01356	0.00289	0.0121	0.0019	0.0016	0.0014	0.0036	0.0069

Location abbreviations: M = Mozambiqueand S = South Africa. Samples Location: 50700 and 50707, Marginal pegmatite, Zaaiplaats and the rest from quartz gold vein in Italy.

Table 2. Analyses of metal-bearing thermal waters in ppm [56]

	Kunashir ***U.S.S.R.***	**Steamboat** ***Nevada***	**Broadlands** ***New Zealand***	**Salton Sea** ***California***	**Matsao** ***Taiwan***
CO_2(species)		410	121	150	10
Na	514	635	711	50400	5560
K	59.4	77	142	17500	930
Cs	0.12		1.15	14	9.6
Ca	137.9	7.9	1.49	28000	1530
Mg	57.1	0.01	0.07	54	135
Fe(species)	95.7	0.02	0.36	2290	160
Mn	11.6	0.01	0.013	1400	43
Al	29.6	0.01		4.2	1.4
Li	0.80	7.3	7.39	215	29
Sr		1.4		400	
Ba		0.11		235	
Cu	0.03	0.003	0.0009	8	0.05
Zn	3.2	0.048	0.001	540	11
Pb	0.36	0.026	0.0013	102	0.7
As	3.0	3.5	5.7	12	4.2
B	22.5	45	133	390	112
Cl	1468	835	1181	155000	13300
Br			3.9	120	
F	2.7	2.2	4.94	15	6.7
SO_4(species)	1476	107	5.4	5.4	305

Table 3. Log K values for reactions calculated for 185°C and 1 kb, using the SUPCRT92 program with addition data from Zotov *et al.* [63] and Benning and Seward [5]

1)	$2As_2S_3 + 2H_2O = As_4S_4 + 2H_2S + O_2$	logK = −48.896
2)	$2As_2S_3 + 2H_2O = As_4S_4 + 2HS^- + 2H^+ + O_2$	logK = −61.602
3)	$2As_2S_3 + 2H_2O + 3O_2 = As_4S_4 + 2SO_4^{2-} + 4H^+$	logK = 92.706
4)	$As_2O_3 + 3HS^- + 3H^+ = As_2S_3 + 3H_2O$	logK = 32.336
5)	$As_2O_3 + 3H_2S = As_2S_3 + 3H_2O$	logK = 13.276
6)	$2As_2O_3 + 4H_2S = As_4S_4 + 4H_2O + O_2$	logK = −22.344
7)	$2As_2O_3 + 4HS^- + 4H^+ = As_4S_4 + 4H_2O + O_2$	logK = 3.069
8)	$2As_2O_3 + 4SO_4^{2-} + 8H^+ = As_4S_4 + 4H_2O + 9O_2$	logK = 305.548
9)	$HSO_4^- = SO_4^{2-} + H^+$	logK = −3.92
10)	$HSO_4^- + H^+ = H_2S + 2O_2$	logK = −74.721
11)	$H_2S = HS^- + H^+$	logK = −6.353
12)	$2O_2 + HS^- = SO_4^{2-} + H^+$	logK = 77.154
13)	$H_2S + 2O_2 = SO_4^{2-} + 2H^+$	logK = 70.801
14)	$As_2O_3 + 3SO_4^{2-} + 6H^+ = As_2S_3 + 3H_2O + 6O_2$	logK = −199.127
15)	$2As_2S_3 + 2H_2O + 3O_2 = As_4S_4 + 2HSO_4^- + 2H^+$	logK = 100.547
16)	$As_2O_3 + 3HSO_4^- + 3H^+ = As_2S_3 + 3H_2O + 6O_2$	logK = −210.888
17)	$2As_2O_3 + 4HSO_4^- + 4H^+ = As_4S_4 + 4H_2O + 9O_2$	logK = −321.229
18)	$Au + 2H_2S + 0.25O_2 = Au(HS)_2^- + 0.5H_2O + H^+$	logK = 4.552
19)	$Au + 2HS^- + H^+ + 0.25O_2 = Au(HS)_2^- + 0.5\ H_2O$	logK = 17.258
20)	$Au + 2SO_4^{2-} + 3H^+ = Au(HS)_2^- + 0.5H_2O + 3.75O_2$	logK = −137.05

In order to examine the effect of pH and fO_2 on the transport and precipitation of As and Au, total arsenic and gold solubilities in a saturated solution of arsenic sulphides or oxide and gold were calculated as a function of pH and fO_2. Figure 6 is a log molality-pH diagram, representing the total arsenic and gold in a 1.5 m NaCl solution with the $\sum S=10^{-2}$ m, at 185°C and 1 kb. This diagram demonstrates opposing pH effects on gold and arsenic solubility. Arsenic is most soluble at high pH which is coincident with the lowest gold solubility (Fig. 6). Similarly the solubility of gold and arsenic at constant pH (5.5) as a function of fO_2 (Fig. 7), shows that arsenic solubility increases with fO_2 up to $\log fO_2 = -40$, then remains high at higher fO_2, whereas for gold, solubility decreases slowly with decreasing fO_2, down to c. $\log fO_2 = -39$ then increases markedly, due to formation of bisulphide complexes, before decreasing slowly again below $\log fO_2 = -43$.

The log m-pH (Fig. 6) and log m-fO_2 (Fig. 7) diagrams demonstrate that co-transport and co-precipitation of Au and As can not reflect a common response to changes in fO_2 or pH. For example, neutral to slightly acid, oxidizing arsenic-rich fluids cannot transport significant gold.

In order to determine the possible conditions in which arsenic-rich fluids may acquire gold, the sulphur species (H_2S, HS^-, SO_4^{2-}, HSO_4^-) predominance fields and arsenic mineral (As_2S_3, As_4S_4, As_2O_3) stability fields (calculated for $m\sum S$ 10^{-2}m and 10^{-3}m respectively) have been plotted on log fO_2-pH diagrams (Figs. 8 and 9). Since thio-complexes of gold are stable to at least 300°C and probably dominate transport of gold [42,44], contours of gold solubility, have been calculated, as a function of $m\sum S$, pH, fO_2 at 185°C and 1 kb using SUPCRT92 and EQ36NR.

Discussion

Equilibrium factors that affect the solubility, transport and deposition of gold and arsenic include temperature, pressure, pH, fO_2 and availability of ligands.

Temperature; the solubility of gold bisulphide complexes generally increases with increasing temperature under near neutral conditions [5,39]. At low $\sum S$ concentration, the solubilities are nearly constant from 150 to 500°C with a maximum at 200°C. In contrast, orpiment solubility is strongly dependent on temperature [47], for example in near neutral solutions, it is 1.5 orders of magnitude less at 25°C than at 90°C [52].

Pressure; the experimental data over 500 to 1500 bars indicate that at near neutral pH, gold solubility decreases with increasing pressure [5]. High pressure and temperature experimental data are not available for arsenic.

pH; the experimental data indicate that gold is more soluble as the bisulphide complex in neutral to slightly alkaline solution, than in strong acidic or alkaline solutions [42]. The importance of pH is that it controls the gold sulphide speciation. Below pH 5.5, gold occurs as $Au(HS)^0$ and changes in pH will not cause precipitation of gold. However, if $Au(HS)_2^-$ is dominant gold-bearing species (pH > 5.5), both a decrease or an increase in pH may cause gold precipitation.

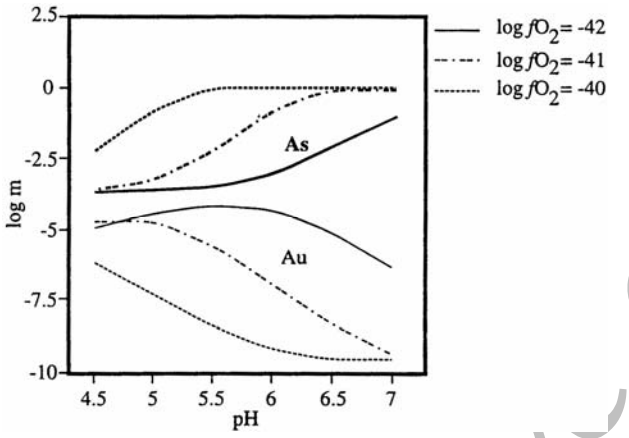

Figure 6. Gold and arsenic total solubility in 1.5 m NaCl and 10^{-2} m ∑S solution, in acid to neutral pH and different oxygen fugacity calculated at 185°C and 1 kb. The diagram shows the opposite effects of pH on arsenic and gold solubility.

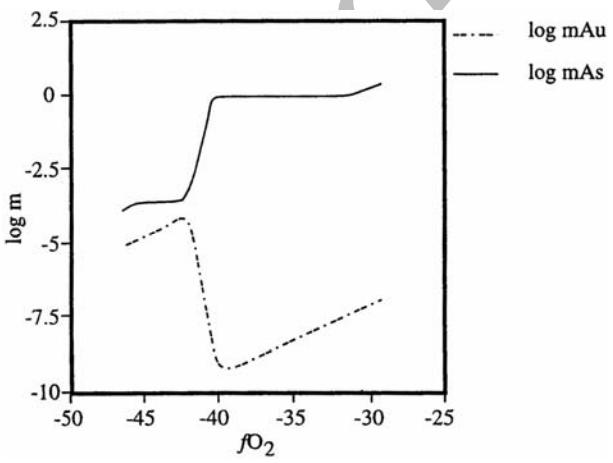

Figure 7. Log m-fO_2 diagram showing the effect of oxygen fugacity on total Au and As solubility at constant pH (5.5), in 1.5 m NaCl and 10^{-2} m ∑S solution at 185°C and 1 kb.

Orpiment solubility is independent of pH changes in acid conditions [39], but at pH > 5.5 As concentration in the fluid increases systematically with increasing pH (Fig. 6).

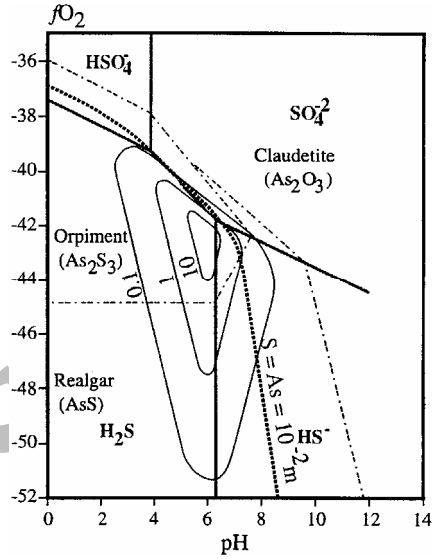

Figure 8. fO_2-pH diagram at 185°C and 1kb showing the stability field of the principal sulphur species, arsenic minerals, and solubility contours for gold in ppm as $Au(HS)_2^-$ for m∑S = 10^{-2}. The heavy dash line shows equal As and S molality.

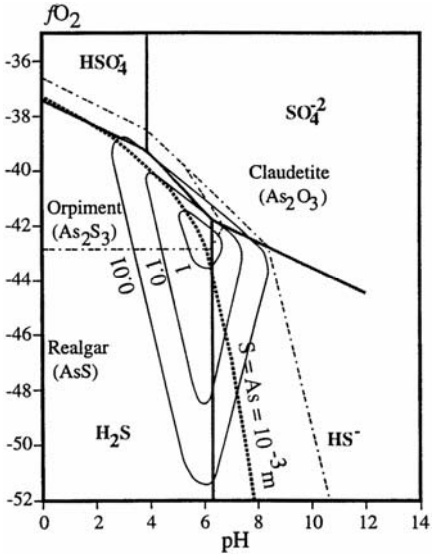

Figure 9. fO_2-pH diagram at 185°C and 1kb showing the stability field of the principal sulphur species, arsenic minerals, and solubility contours for gold in ppm as $Au(HS)_2^-$ for m∑S = 10^{-3}. The heavy dash line shows equal As and S molality.

fO_2; regardless of whether gold is transported as a chloride complex or sulphide complex, decrease in fO_2 is an effective mechanism for gold precipitation over most fO_2 ranges (see Figs. 6 and 7). However there is a marked increase in Au solubility in S-bearing solutions on passing from the sulphate predominance field to the fields of reduced S species predominance (Fig. 7). Arsenic solubility increases regularly with fO_2, irrespective of S-speciation, so that the two show opposite trends in the critical region near the sulphate-sulphide predominance boundary.

H_2S loss; if gold is transported in hydrothermal solution as a bisulphide complexes, loss of H_2S from fluid causes gold precipitation (see Equation 1). A decrease in H_2S content may be caused by boiling, by sulphide mineral precipitation or by mixing with H_2S-poor solutions (*e.g.* shallow ground water).

Gold solubility increases with increasing total dissolved sulphur (Fig. 8), with the maximum solubility of Au (as $Au(HS)_2^-$) recorded where pH=pK_1 of H_2S [5,42]. As the amount of dissolved sulphur in arsenic-rich fluid may have an important role on gold solubility, pH and fO_2 for mAs=mS were calculated by EQ36NR (heavy dash line in Fig. 8 and Fig. 9). The logic for this, was to evaluate the effect of the large scale removal of S from solution as orpiment on gold solubility. The main question is to find a condition in which the arsenic-rich fluid can acquire significant gold, and keeping sulphur in the system is vital to achieve that.

It is not one factor which causes metal transport and precipitation from the solution, but a mixture of independent factors which may differ from deposit to deposit. Although pH and fO_2 exercise an important control on gold and arsenic solubility, the changes on pH and fO_2 cannot result directly in gold and arsenic co-precipitation because the effects are opposed on their solubilities [47].

Equation 1 is the principal reaction controlling the solubility and transport of gold at neutral to weakly acid, reducing conditions. This reaction indicates that in addition to changes in pH and fO_2 (Fig. 7) any process which decreases m$\sum$S will precipitate gold. Hence sulphide loss alone can be a very effective means of gold deposition, as indicated by Reed and Spycher [34] and Spycher and Reed [46].

$$Au(HS)_2^- + H^+ + 0.5\ H_2O = Au + 0.25O_2 + 2H_2S \quad (1)$$

Equation 2 is the reaction that controls orpiment deposition at similar pH and fO_2. Although orpiment solubility is strongly depending on temperature [47], sulphide concentration (and pH) also has an important influence.

$$2H_3AsO_{3(aq)} + 3H_2S = As_2S_3 + 6H_2O \quad (2)$$

Comparison of the two reactions shows that, despite the opposing pH effects, a possible connection between As and Au precipitation is that orpiment precipitation will reduce the S level in solution, which, if As is at compatible levels to S, will in turn promote gold precipitation. Thus a possible cause of co-precipitation in fluids with As levels comparable to H_2S concentrations would be a change in intensive parameters leading to orpiment precipitation, which would in turn drive gold precipitation by removing S from the fluid.

The critical factor is then the arsenic:sulphide ratio in the ore-forming fluid, because if S is in excess in comparison to arsenic, arsenic precipitation is likely accompanied by increase in gold solubility and orpiment precipitation will not have a significant effect. If the m$\sum$S is equal to or less than mAs, then precipitation of orpiment decreases the sulphur level in the ore-forming fluid and results in a decrease in gold solubility, destabilizing gold sulphide complexes.

Figures 8 and 9 are fO_2-pH diagrams at 185°C and 1 kb showing the stability fields of the principal sulphur species, arsenic minerals and solubility contours for gold in ppm as $Au(HS)_2^-$ for $\sum S = 10^{-2}$ and 10^{-3} m, imposed by equal As-S molality line. Comparison of Figure 8 and Figure 9 shows that for mAs=mS= 3×10^{-3} a high level of As, *i.e.* As ~ S, coincides with the highest gold solubility (1 ppm contour) and from this point onward decrease in sulphur concentration (orpiment precipitation), or fO_2, or changes in pH will result in drop in gold solubility and gold precipitation.

Kinetic Effect

An alternative control on the co-precipitation of As and Au is a kinetic one. Experimental study of gold adsorption onto mineral surfaces has been reviewed by Renders and Seward [36], Hyland and Bancroft [17], Schoonen *et al.* [41], Knipe *et al.* [21], Mycroft *et al.* [31] and Maddox *et al.* [23]. The adsorptive capability largely depends on the nature of adsorbate (mineral), adsorbent (solution) and the species of gold in solution. In general, sulphides have larger adsorption potential than oxides, carbonates and probably silicate [17,41]. Most of the studies focused on pyrite, arsenian-pyrite and arsenopyrite.

The adsorption of gold by As_2S_3 and Sb_2S_3 has been suggested by Seward [43] and Renders and Seward [36] as a precipitation mechanism for gold found in active hydrothermal systems. The experimental studies indicate that As_2S_3 adsorbs up to four times more gold

than Sb_2S_3 at the same pH and $m_{Au,t}$ [36]. They concluded that once arsenic and antimony sulphides have started to precipitate, they will continue to concentrate gold until their surfaces have become saturated at that particular gold concentration. An important point is that adsorption by As_2S_3 or Sb_2S_3 will cause the removal of gold from solutions considerably undersaturated with respect to gold or a gold-rich compound. Thus adsorption provides an alternative mechanism to explain Au-As association to S-removal model outlined in the previous section. It is of proven effectiveness and likely to be important in relatively low As deposits, *i.e.* those lacking orpiment and realgar.

Applications to the Zarshuran Deposit

It follows from Figure 6 that co-precipitation of arsenic and gold is not a matter of simple lowering of the solubility of both metals. The metals may have been carried in a single fluid which dissolved gold by leaching at conditions near to the gold solubility maximum or in different fluids. Co-precipitation may have occurred by reduction of a single fluid by black shale or by mixing of As-rich and Au-rich fluids. Based on geological and geochemical modelling data, two possible scenarios can be proposed for gold and arsenic co-precipitation at Zarshuran, single fluid model and mixing model.

Single Fluid Model

In a single fluid model, a probably magmatic fluid is considered to provide the main mass contribution, but it may behave chemically in two possible ways:

A single fluid equilibrium model

In this model, an oxidized As- and S-rich fluid may have been contributed directly from magmatic activity. In order to acquire gold, the fluid must have been partially reduced to leach significant amount of gold. Partial reduction by and leaching of, Precambrian metamorphic rocks, may have provided the gold. Subsequent more extreme reduction of the fluid due to reaction with organic-rich shale, which acted as a geochemical barrier, provided the environment for deposition of orpiment and gold. Comparison between Figures 8 and 9 indicates that the concentration of S and As:S ratio are vital controls on this model. As shown in Figure 9, only at As~S and $\sum S$ 10^{-3}m does the original As-rich fluid meet the condition of having S available to dissolve significant gold (compare the position of heavy dash line and gold solubility contours in Fig. 9), while comparable levels of As remain in solution. From this point onward decrease in pH and fO_2 will result in precipitation of orpiment from this fluid (As~S, and $\sum S$ of 10^{-3}m), and the resulting loss in S will then promote gold precipitation.

A single fluid disequilibrium model

In this model, an oxidized As- and S-rich fluid is partially reduced and leaches gold from the metamorphic rocks, before co-precipitating gold and arsenic sulphide in the extremely reduced, organic-rich shale. However the main precipitation process for gold is surface adsorption without gold supersaturation. As it is in a disequilibrium condition, the As:S ratio and $\sum S$ are not critical and gold concentration could be below saturation. Adsorption/reduction of gold complexes on sulphide minerals is considered to be an effective mechanism for gold deposition, especially at low gold content and relatively low temperature [19,37]. The variability in the EPMA gold analyses of sulphide minerals [24] supports the possibility of surface adsorption as a depositional process during the mineralization.

Fluid Mixing Model

Since significant gold and arsenic are not readily transported together, (Figs. 6 and 7), the existence of two different fluids, an oxidized, As-rich and a reduced, Au-rich fluid, with mixing in a suitable environment, provides another possible scenario. In this model, the host rock should be physically able to provide the mixing environment and the chemistry of host rock probably is not as important as in the single fluid models. Fluid inclusion data support the presence of at least two fluids during the mineralization, though clarifying the source(s) of these fluids requires more detailed work. Presence of very low salinity and low temperature aqueous fluid, interpreted as a meteoric water end-member, which by entering deep zone become more and more reducing, particularly as the surrounding rocks contain significant amount of organic matter and sulphides. This reduced fluid probably leaches Au from the Precambrian basement and flow through the contact of sedimentary rock cover and basement. However condensation of volcanic gases into meteoric waters to introduce volatiles is a possibility. On the other hand mixing could be considered as a destabilizing factor for mineral deposition from a dominantly magmatic ore fluid.

The spatial and temporal association of mineralization with magmatic activity and the fluid inclusion evidence for As- and S-rich pegmatite fluids [33], suggest that a magmatic fluid could provide the

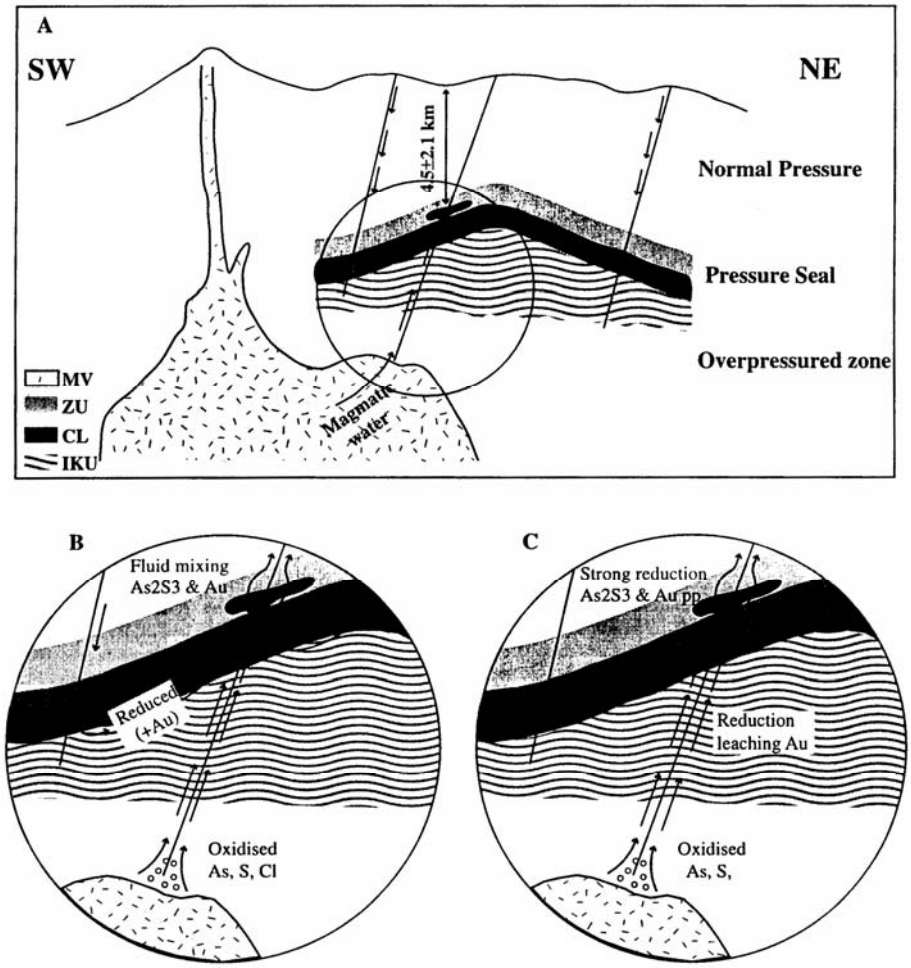

Figure 10. Schematic model for the development of Zarshuran deposit. Abbreviations: MV, Miocene Volcanics; ZU, Zarshuran Unit (black shale); CL, Chaldagh Limestone, and IKU, Iman Khan Unit (greenschist). The ringed area in part (a) is shown in detail in (b) and (c) which illustrate two separate models. b) illustrate a two-fluid model in which mineralisation results from mixing of an oxidized As-rich fluid with a reduced Au-bearing fluid, while c) a single magmatic fluid leaches Au as it is reduced by interaction with wall rocks, before co-precipitating Au and as in the Zarshuran black shale.

metals and sulphur to make this model viable. The average gold concentration of 384 ppb [49] in the Iman Khan Unit, would facilitate the partial reduction and indicates that the original fluid could acquire significant gold by leaching.

The fluid mixing model is supported by fluid inclusion data and the strict chemical condition of As and Au co-transportation, but it does not account for the importance of the geochemical barrier, organic-rich shale, in controlling mineralization. The mineralization in this scenario could have happened in any environment which physically provides suitable porosity and permeability for fluid mixing. However considering the Zarshuran Unit as pressure seal, with throttling of fluid(s), causing abrupt pressure decrease and fluid expansion, as discussed by Toulmin and Clark [51], may justify the localization of the ore deposit in this unit, on primarily physical grounds.

Summary and Conclusions

Figure 10 is a schematic diagram illustrating a possible environment for mineralization at the Zarshuran deposit. By using the estimated physical conditions and the proposed geochemical models, it is possible to encompass depth of formation, restriction of mineralization to black shale, presence of wide range of fluid inclusion types, fluctuation in pressure and tempe-

rature, the strong correlation between Au and As and the high gold value in orpiment veins (arsenical ore) in the Zarshuran deposit. This may be applicable to other such sediment-hosted disseminated gold deposits. However, in some cases the source(s) of fluid and metal is conjectural and need to be strengthened by more work.

In this model, Zarshuran Black Shale acted as a pressure seal and an extreme redox geochemical barrier. Therefore faults, or the Iman Khan anticline axis are the most likely causes of leakage from the overpressured environment. A deep hot overpressured oxidized As- and S-rich fluid would ascend along fractures and acquire Au either by partial reduction through metamorphic basement or mixing with a reduced Au-bearing fluid and move toward the site of ore body at paleodepth of 4.5±2.1 km.

Sharp [45], Cathles and Smith [7], and Christensen *et al.* [8] proposed an episodic basin dewatering mechanism for the genesis of the Mississippi Valley-type lead-zinc deposits, which is comparable to episodic discharge from sealed compartment in some of the basins [16]. These studies therefore provide a basis for the model illustrated in Figure 10.

It is highly possible that fluid in the overpressured compartment had enough time to equilibrate with surrounding rocks. Therefore partial reduction of oxidized As- and S-rich magmatic fluid and leaching of gold may provide an arsenic-rich gold-bearing fluid with further reduction by organic-rich shale resulting in gold and arsenic co-precipitation. The co-precipitation may either facilitated by equilibrium factors or kinetic effects.

The episodic nature of the process resulted in changes in fluid flow rate, pressure and chemistry of fluid at every break out, which shifted the deposition locus, the type of mineral precipitated and the nature of the trapped fluid inclusions in a very complex manner. The result would be a complex paragenesis and zoning and wide range of fluid inclusions within individual samples, as observed in Zarshuran deposit. In addition to abrupt pressure drop, several chemical processes may occur in the mixing environment which can lead to mineral deposition, notably dilution; changes in pH and fO_2, and cooling. In fact they may have occurred simultaneously, but more detailed work is required in order to refine deep fluid mixing.

Acknowledgements

For their assistance in the analytical aspects, we would like to thank, Dave Banks (fluid inclusion studies), Eric Condliffe (EPMA and SEM) and Geoff Lloyd (SEM).

References

1. Akinfiev N.N., Zotov A.V., and Nikonorov A.P. Thermodynamic analysis of equilibria in the As(III)-S(II)-O-H system. *Geochemistry International*, **29**: 109-21 (1992).
2. Arehart G.B., Chryssoulis S.L., and Kesler S.E. Gold and arsenic in iron sulfides from sediment-hosted disseminated gold deposits: Implication for depositional processes. *Econ. Geol.*, **78**: 171-185 (1993).
3. Asadi H.H. The Zarshuran gold deposit model applied in a mineral exploration GIS in Iran. PhD thesis, ITC, Netherland, Dissertation No. **78**: ISBN 90-6164-1853 (2000).
4. Barnicot A.C., Henderson I.H.C., Knipe R.J., Yardley B.W.D., Napier R.W., Fox N.P.C., Kenyon A.K., Muntingh D.J., Strydom D., Winkler K.S., Lowrence S.R., and Cornfords C. Hydrothermal gold mineralisation in the Witwatersarand basin. *Nature*, **386**: 820-824 (1997).
5. Benning L.G. and Seward T.M. Hydrosulphide complexing of Au(I) in hydrothermal solutions from 150-400°C and 500-1500 bar. *Geochim. Cosmochim. Acta*, **60**: 1849-1871 (1996).
6. Boyle R.W. The geochemistry of gold and its deposits. *Geol. Surv. Canada Bull.*, **280**: 584 (1979).
7. Cathles L.M. and Smith A.T. Thermal constraint on the formation of Mississippi Valley-type lead-zinc deposits and their implication for episodic basin dewatering and deposit genesis. *Econ. Geol.*, **78**: 983-1002 (1983).
8. Christensen J.N. *et al.* Testing models of large-scale crustal fluid flow using direct dating of sulphides: Rb-Sr evidence for early dewatering and formation of Mississippi Valley-Type deposits, Canning Basin, Australia. *Econ. Geol.*, **90** 877-884 (1995).
9. Ellis A.J. and Giggenbach W. Hydrogen sulphide ionisation and sulphur hydrolysis in high temperature solution. *Geochim. Cosmochim. Acta*, **35**: 247-260 (1971).
10. Engelder T. and Lacazette A. Natural hydraulic fracturing. *In:* Barton, N. and Stephansson, O. (eds.), Rock joints. Rotterdom, A.A. Balkema, 35-43 (1990).
11. Gammons C.H. and Williams-Jones A.E. The solubility of Au-Ag alloy + AgCl in HCl/NaCl solutions at 300°C: New data on the solubility of Au(I) chloride complexes in hydrothermal fluids. *Geochim. Cosmochim. Acta*, **59**: 3453-3468 (1995).
12. Gretener P.E. Pore pressure: Fundamentals, general implications for structural geology. *Amer. Asso. Petrol. Geologists, Education Course Note Series*, **4**: 131 p. (1981).
13. Hayashi K. and Ohmoto H. Solubility of gold in NaCl- and H_2S-bearing aqueous solutions at 250-350C. *Geochim. Cosmochim. Acta*, **55**: 2111-2126 (1991).
14. Helgeson H.C., Delaney J.M., Nesbitt H.W., and Bird D.K. Summary and critique of the thermodynamic properties of rock forming minerals. *Amer. Jour. Sci*, **278A**: 1-229 (1978).
15. Henley R.W. The solubility of gold in hydrothermal chloride solution. *Chem. Geol.*, **11**: 622-635 (1973).
16. Hunt J.M. Generation and migration of petroleum from

abnormally pressure fluid compartments. *AAPG Bulletin*, **79**(1): 1-12 (1990).
17. Hyland M.M. and Bancroft G.M. An XPS study of gold deposition at low temperature on sulfide minerals:Reducing agent. *Geochim. Cosmochim. Acta*, **53**: 367-372 (1989).
18. Ivakin A.A., Vorob'va S.V., Gorelov A.M. and Gertman E.M. Solubility of arsenic sulphide (III) sulphide in aqueous NaCl solutions. *Russian Journal of Inorganic Chemistry*, **24**: 1089-1091 (1979).
19. Jean G.E. and Bancroft G.M. An XPS and SEM study of gold deposition at low temperatures on sulfide mineral surfaces: concentration of gold by adsorption / reduction. *Geochim. Cosmochim. Acta*, **49**: 979-987 (1985).
20. Johnson J.W., Oelkers E.H., and Helgeson H.C. SUPCRT92, A software package for calculating the standard modal thermodynamic properties of mineral, gases, aqueous species, and reaction from 1 to 5000 bars and 0° to 1000°C. *Comput. Geosci.*, **18**: 899-947 (1992).
21. Knipe S.W., Scaini M.J., and Bancroft G.M. Gold sorption on pyrite from bisulphide solution, at 25-90 degrees C; surface chemical and textural analysis. *Geological Association of Canada, Joint Annual Meeting, Program with Abstract*, **20**: pages 53 (1995).
22. Krupp R.E. and Seward T.M. The Rotokawa geothermal system, New Zealand,: An active epithermal ore-deposition environment. *Econ. Geol.*, **82**: 1109-1129 (1987).
23. Maddox L.M., Bancroft G.M., Scaini M.J., and Lorimer J.W. Invisible gold: comparison of gold deposition on pyrite and arsenopyrite. *Am. Miner.*, **83**: 1240-1245 (1998).
24. Mehrabi B. Genesis of the Zarshuran gold deposit, NW Iran. Unpublished PhD thesis, University of Leeds (1997).
25. Mehrabi B., Yardley B.W.D., and Cann J.R. Sediment-hosted disseminated gold mineralization at Zarshuran, NW Iran, *Mineralium Deposita*, **34**: 673-696 (1999).
26. Mernagh T.P. *et al.* Chemistry of low-temperature hydrothermal gold, platinum, and palladium (±uranium) mineralisation at Coronation Hill, Northern Territory, Australia. *Econ. Geol.*, **89**: 1053-1073 (1994).
27. Mironova G.B. and Zotov A.V. Solubility studies of the stability As(III) sulphide complexes at 90°C. *Geochemistry International*, **17**(2): 46-54 (1980).
28. Mironova G.B., Zotov A.V., and Gul'ko N.I. Determination of the solubility of orpiment in acid solution at 25-150°C. *Geochemistry International*, **21**(1): 53-59 (1984).
29. Mironova G.B., Zotov A.V., and Gul'ko N.I. The solubility of orpiment in acid solution at 25-150°C and the stability of arsenic sulphide complexes. *Geochemistry International*, **27**(12): 61-73 (1990).
30. Mohajer Gh., Parsaie H., Fallah N., and Ma'dani F. Mercury exploration in the Saein Dez- Takab. *IIMRA*, Tehran, (in Farsi) (1989).
31. Mycroft J.R., Bancroft G.M., McIntyre N.S., and Lorimer J.W. Spontaneous deposition of gold on pyrite from solution containing Au(III) and Au(I) chlorides, Part 1, a surface study. *Geochim. Cosmochim. Acta*, **59**: 3351-3365 (1995).
32. Nakagawa R. Solubility of orpiment (As_2S_3) in Tamagawa hot springs, Akita Prefecture (in Japanese). *Nippon Ngako Zasshi*, **92**: 154-159 (1971).
33. Pike S. The chemistry of granite derived pegmatite fluids. Unpublished PhD thesis, University of Leeds (1992).
34. Reed M.H. and Spycher N.F. Boiling, cooling, and oxidation in epithermal system, A numerical modelling approach. *Rev. in Econ. Geol.*, **2**: 249-272 (1985).
35. Renders P.J. and Seward T.M. The stability of hydro-sulphido and sulphido-complexes of Au(I) and Ag(I) at 25°C. *Geochim. Cosmochim. Acta*, **53**: 245-253 (1989a).
36. Renders P.J. and Seward T.M. The adsorption of thio gold(I) complexes by amorphous As_2S_3 and Sb_2S_3 at 25 and 90°C. *Geochim. Cosmochim. Acta*, **53**: 255-267 (1989b).
37. Ridley J., Mikucki E.I., and Groves D.I. Archean lode-gold deposits: fluid flow and chemical evolution in vertica extensive hydrothermal systems. *Ore Geology Reviews*, **10**: 279-293 (1996).
38. Rytuba J.J. Mutual solubilities of pyrite, pyrrhotite, quartz and gold in aqueous NaCl solution from 200 degrees to 500 degrees C, and 500-1500 bars, and genesis of the Cortez gold deposit, Nevada. *GSA* 78-105787 (1977).
39. Rytuba J.J. Geochemistry of hydrothermal transport and deposition of gold and sulfide minerals in Carlin-type gold deposits. *In:* Tooker E.W. (Ed.), Geological characteristics of sediment- and volcanic-hosted disseminated gold deposit- Search for an occurrence model. *USGS Bull.*, **1646**: 27-34 (1985).
40. Samimi M. Recognisance and preliminary exploration in the Zarshuran, *Kavoshgaran Eng. Consultant*, Tehran (in Farsi) (1992).
41. Schoonen M.A.A., Fisher N.S., and Wente M. Au sorption onto pyrite and goethite: a radiotracer study (1992).
42. Seward T.M. Thio complexes of gold and the transport of gold in hydrothermal solutions. *Geochem. Cosmochem. Acta*, **37**: 379-399 (1973).
43. Seward T.M. The transport and deposition of gold in hydrothermal system, *In:* Forster R.P. (Ed.), *Gold'82*, The geology, geochemistry, and genesis of gold deposits. 165-181, A.A. Blackman (1984).
44. Seward T.M. The hydrothermal geochemistry of gold. *In:* Forster R. P. (Ed.), Gold Metallogeny and Exploration, Chap. 2, 37-62, Blakie (1991).
45. Sharp J.M. Energy and momentum transport model of the Ouachita basin and its possible impact on the formation of economic mineral deposits. *Econ. Geol.*, **73**: 1057-1068 (1978).
46. Spycher N.F. and Reed M.H. Boiling of geothermal waters, Precipitation of base and precious metals, speciations of arsenic and antimony, and the role of gas phase metal transport, *In:* Jackson K. and Bourccier W. (Eds), Proceedings of the workshop on geochemical modelling, Fallen Leaf Lake, September 1986, Livermore, California, *Lawrence Livermore National Laboratory*, CONF-8609134 (1986), P. 58-65 (1986).
47. Spycher N.F. and Reed M.H. Evolution of a Broadland-Type epithermal ore fluid along P-T paths: Implication for the transport and deposition of base, precious, and volatile metals. *Econ. Geol.*, **84**: 328-359 (1989).

48. Stocklin J. Structural history and tectonics of Iran: A review, *American Association of Petroluem Geologist (AAPG) Bulletin*, **52**: 1229-1258 (1968).
49. Taddaion A.H. Detailed geochemical prospection in Zarshuran mine area, Takab, Ministry of Mines and Metals, Zarshuran gold project, 79 p. (in Farsi) (1991).
50. Thompson J.F.H. *et al.* Cu-Au metallogeny of alkalic arc magmatism: Examples from the Mesozoic arc terranes of the northern Canadian Cordillera and comparison to the Tabar-Feni arc, *In:* Clark A.H. (Ed), Giant Ore Deposits-II, Queens University, Kingston, Ontario, 668-673 (1995).
51. Toulmin P. and Clark S.P. Thermal aspects of ore formation. *In:* Barnes H.L. (Ed.) Geochemistry of hydrothermal ore deposits. New York, Holt, Rhinehart and winston, 437-464 (1967).
52. Webster J.G. The solubility of As_2S_3 and speciation of As in dilute and sulphide-bearing fluids at 25 and 90°C. *Geochem. Cosmochem. Acta*, **54**: 1009-117 (1990).
53. Weissberg B.W. Gold-silver ore-grade precipitates from New Zealand thermal waters. *Econ. Geol.*, **64**: 95-108 (1969).
54. Wells J.D. and Mullens T.E. Gold-bearing arsenian pyrite determined by microprobe analysis, Cortez and Carlin gold mines, Nevada. *Ibid.*, **68**: 187-201 (1973).
55. White D.E. Mercury and base-metal deposits with associated thermal and mineral waters. *In:* Barnes N. L. (Ed.), Geochemistry of hydrothermal ore deposits, New York, Holt, Rinehart and Winston, p. 575-631 (1967).
56. White D.E. Active geothermal systems and hydrothermal ore deposits. *Econ. Geol.*, 75th Anniv. Vol., 392-423 (1981).
57. Wolery T.J. Calculation of chemical equilibrium between aqueous solution and minerals- the EA3/6 soft-ware package, UCRL-52658, Berkeley, University of California, *Lawrence Livermore National Laboratory*, 41 p. (1979).
58. Wolery T.J. EQ3NR, A computer program for geochemical aqueous speciation-solubility calculations, User's guide and documentation, UCRL-53414, Berkeley, University of California, *Ibid.*, 191 p. (1983).
59. Wolery T.J. EQ6, A computer program for reaction path modeling aqueous geochemical system, User's guide and documentation:UCRL-51, Berkeley, University of California, *Ibid.*, 251 p. (1984)
60. Wolery T.J. and Daveler S.A. EQ3/6, A computer program for reaction-path modelling of aqueous system, UCRL-MA-110772 PT I-IV, Berkeley, University of California, *Ibid.* (1992)
61. Wolery T.J., Sherwood D.J. Jackson K.J., Delaney J.M., and Puigdimenech I. EQ3/6, Status and applications, UCRL-91884, Berkeley, University of California, *Ibid.*, 12 p. (1984)
62. Yardley B.W.D., Banks D.A., Bottrell S.H., and Diamond L.W. Post-metamorphic gold-quartz veins from N.W. Italy: the composition and origin of the ore fluid. *Min. Mag.*, **57**: 407-422 (1993).
63. Zotov A.V., Kudrin A.V., Levin K.L. Shikina N.D., and Var'yash L.N. Experimental studies of the solubility and complexing of selected ore elements (Au, Ag, Cu, Mo, As, Sb, Hg) in aqueous solutions, *In:* Shmulovich K.I., Yardley B.W.D., and Gonchar G.G. (Eds.), Fluids in the Crust equilibrium and transport properties, Chapman and Hall, London, p. 95-139 (1995).